Dong Han
Department of Surgery,
University of Maryland School of Medicine,
10 South Pine Street, MSTF 436,
Baltimore, MD 21201

Jiafeng Zhang
Department of Surgery,
University of Maryland School of Medicine,
10 South Pine Street, MSTF 436,
Baltimore, MD 21201

Bartley P. Griffith
Department of Surgery,
University of Maryland School of Medicine,
10 South Pine Street, MSTF 436,
Baltimore, MD 21201

Zhongjun J. Wu[1]
Department of Surgery,
University of Maryland School of Medicine,
10 South Pine Street, MSTF 436,
Baltimore, MD 21201;
Fischell Department of Bioengineering,
A. James Clark School of Engineering,
University of Maryland,
College Park, MD 20742
e-mail: zwu@som.umaryland.edu

Models of Shear-Induced Platelet Activation and Numerical Implementation With Computational Fluid Dynamics Approaches

Shear-induced platelet activation is one of the critical outcomes when blood is exposed to elevated shear stress. Excessively activated platelets in the circulation can lead to thrombus formation and platelet consumption, resulting in serious adverse events such as thromboembolism and bleeding. While experimental observations reveal that it is related to the shear stress level and exposure time, the underlying mechanism of shear-induced platelet activation is not fully understood. Various models have been proposed to relate shear stress levels to platelet activation, yet most are modified from the empirically calibrated power-law model. Newly developed multiscale platelet models are tested as a promising approach to capture a single platelet's dynamic shape during activation, but it would be computationally expensive to employ it for a large-scale analysis. This paper summarizes the current numerical models used to study the shear-induced platelet activation and their computational applications in the risk assessment of a particular flow pattern and clot formation prediction. [DOI: 10.1115/1.4052460]

1 Introduction

Platelets play an essential role in physiological hemostasis, a natural process for preventing excessive blood loss from a damaged blood vessel [1,2]. The resting platelet has a stable discoid shape that is circulating in the bloodstream. Platelets adhere and aggregate to damaged endothelium, instantaneously followed by the activation of platelets that triggers the secondary hemostasis. A platelet plug is formed, and then platelets degranulate [3]. During their lifespan, platelets are continuously subjected to mechanical shear stress in the circulation. While physiological shear stresses in the circulatory system do not have a detrimental impact on blood cells, platelets exposed to elevated shear stresses, such as in blood flow through a stenotic blood vessel, exhibit structural and functional alterations [4–6]. One of these alterations is platelet activation. Similarly, the complex blood flow with higher shear stress in medical devices can irreversibly induce platelet activation. These activated platelets adhere and aggregate on the foreign surface of medical devices, promoting clot growth that could be a potential life threat to patients. Thrombus growth is a very complex process involving physical, chemical, and physiological interactions. Thus, platelet activation induced by nonphysiological shear stress becomes the most critical concern in clinical use of medical devices.

Computational fluid dynamics (CFD) modeling has been a helpful engineering tool to study the blood flow patterns in medical devices over the past two decades [7–10]. It can provide a detailed insight into fluid flow information inside the vasculature or blood-contacting medical devices (BCMDs). The CFD modeling can be further used to achieve optimized flow characteristics based on minimizing high shear stress regions. Incorporated with the CFD modeling, power-law models that relate hemolysis to shear stress and exposure time have been widely used to evaluate red blood cell (RBC) damage caused by medical devices [11,12]. The power-law models are also adapted to evaluate the potential of shear-induced platelet activation [13–16]. Several modified models have been proposed to improve the performance of the original power-law model when implemented in the CFD simulation [17–20]. For example, the linear power-law model becomes popular due to its simple formula [17]. The cumulative model is adapted from the damage accumulation, which considers the shear stress accumulation effect on a single platelet [21]. Furthermore, the Eulerian form of the cumulative model is flexible to be adopted in the clot growth simulation [19,22]. The threshold model also classifies whether a platelet is activated or not, comparing the shear stress (shear rate) experiences to a threshold value [23].

The classical power-law-like models require empirical/ad hoc parameters dependent on the device and operating conditions. Therefore, they have limited success and can hardly be considered a universal approach for predicting shear-induced platelet activation. The multiscale platelet model based on the molecular structure is a promising approach to reveal the shear-induced platelet activation, yet it is too complex and computationally expensive to be applied for problems on larger scales [24,25]. Recently, a continuum macroscale RBC model combined with a microscale membrane structure model has been developed to investigate the RBC damage due to leakage of hemoglobin from ruptured membrane pores on the deformed membrane [26]. A similar approach may be utilized to model the shear-induced platelet activation by investigating the mechanical response of a single platelet to shear stress. However, the challenge arises due to the dramatically morphological change of platelet's structure during activation, usually accompanied by a sequence of complex biochemical reactions.

2 Background

2.1 Platelet Function and Coagulation Cascade. Platelets, or thrombocytes, are small anucleate cells circulating in the blood.

[1]Corresponding author.
Manuscript received July 9, 2021; final manuscript received September 8, 2021; published online November 5, 2021. Assoc. Editor: Ethan Kung.

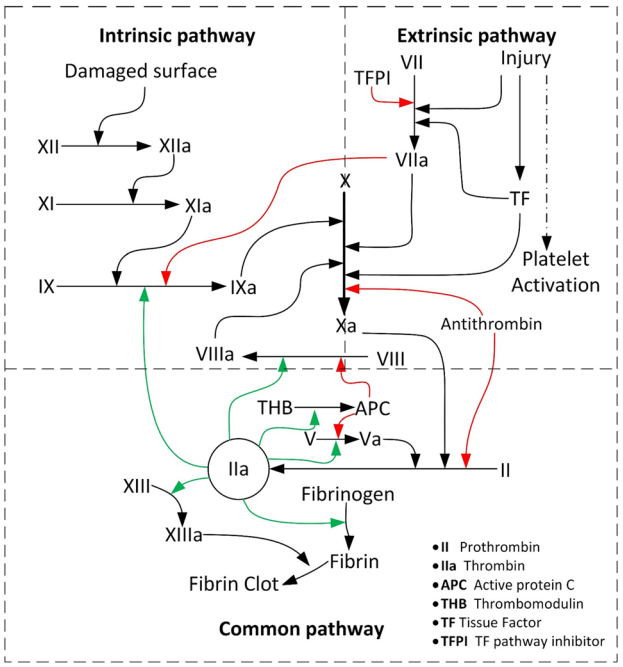

Fig. 1 Coagulation cascade. Green arrows stand for the amplification effects, and red arrows stand for inhibition effects. (Color version online.)

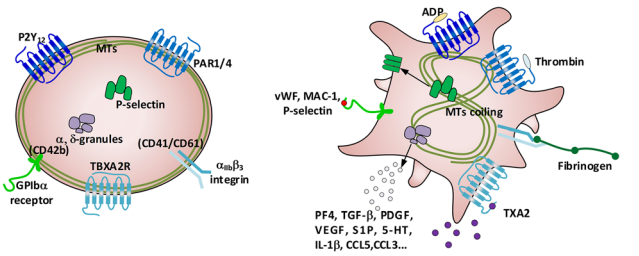

Fig. 2 A simplified platelet scheme from resting state to activation. A resting platelet has a stable discoid shape balanced by its membrane and MTs. The membrane surface is coupled with G-protein coupled receptors that can bind several ligands resulting in decreased intracellular cyclic adenosine monophosphate, mobilization of Ca^{2+} stores. Upon activation, MTs coils and leads the platelet morphological change to a spiny sphere. Soluble granule proteins are released. Membrane proteins retained in the granules are mobilized and presented at the cellular surface where they can bind related ligands.

They are fragments of cytoplasm derived from megakaryocytes, which are large cells produced from stem cells in the bone marrow [27]. The principal function of platelets is to initiate the primary hemostasis through a complex activation process at the site of vascular injury. When platelets contact the exposed subendothelium at the injury site, adhesion receptors (GPVI, GPIb, and integrin $\alpha 2\beta 1$) on the platelet bind collagen and von Willebrand factor (vWF) from the subendothelium, triggering a sequence of cellular events in adhered platelets, leading to platelet activation. A sequence of coagulation events (secondary hemostasis) follows, leading to platelet/fibrin crosslinked clot formation. Platelet can also be activated via exposure to chemical and mechanical stimuli known as the agonist. Those agonists include adenosine diphosphate (ADP), thrombin, thromboxane A2 (TXA2), epinephrine, serotonin, collagen, shear stress, prostaglandin E_2, and 8-iso-prostaglandin $F_{2\alpha}$. In addition, activated platelets release several biologically active substances stored in their granule contents, including ADP, serotonin, platelet-activating factor, vWF, platelet factor 4, and TXA2, into the blood plasma, which, in turn, trigger the activation of more resting platelets [28].

The secondary hemostasis is a rapid process known as coagulation cascade, a complex phenomenon that remains partially understood. It has two initial pathways: intrinsic and extrinsic [29,30], as illustrated in Fig. 1. In the extrinsic pathway, tissue factor from injured subendothelial tissue activates factor VII, which then activates factor X. The biochemical reaction of the intrinsic pathway involves factors XII, XI, IX, and VIII. Finally, the extrinsic and intrinsic pathways merge at the activation of factor X in the common pathway. As a result, thrombin is formed from prothrombin; fibrinogen is converted into fibrin. A complete description of the coagulation cascade model consisting of an initiation phase, amplification phase, and propagation phase can be found in Refs. [30] and [31].

2.2 Platelet Activation. Circulating inactivated platelets have flat, biconvex discoid (lens-shaped) structures. Such a structure is maintained by the membrane and a ring of microtubules (MTs), also known as the marginal band (MB) [32–35]. Upon activation, MB coils and the platelet morphologically changes to a spiny sphere [4,27,28]. Actin filaments are fragmented, which are followed by the dismantling and release of spectrin networks. Then, lamellipodia and filopodia arise from the membrane surface, termed "pseudopodia" [36–38]. Figure 2 shows a simplified representation of the platelet from resting to activated. Besides the structural change, activated platelets undergo functional regulation resulting from the altered expression of surface glycoproteins. Channels of the surface-connected open canalicular system interact with the platelet surface and intracellular storage granules [39]. This inside-out signaling, also known as bidirectional trafficking, increases the number of GPIIb-IIIa complexes and decreases the number of GPIb-IX complexes. The additional conformational change of GPIIb-IIIa complexes results in the exposure of conformation-dependent activation epitopes to their high-affinity ligands, enabling platelet aggregation and clot formation. Mediators, such as ADP, adrenaline, serotonin, thrombin, and TXA2, are secreted from granules in an autocrine and paracrine manner [40]. The release reaction also includes the expression of new granule glycoproteins such as CD62P (P-selectin) or CD63 (a lysosomal glycoprotein), which reflect the activation state of circulating platelets.

2.3 Shear-Induced Platelet Activation and Mediated Aggregation. Although shear stress is conventionally considered a weak agonist in the blood, exposure to fluid shear stress does activate and aggregate platelets irreversibly in the absence of any exogenous agonists [41–45]. Studies using a cone and plate viscometer have demonstrated that platelet could be activated when exposed to relatively elevated fluid shear stress above the physiological level (60 dyn/cm^2) for minutes (60–120 s) [46]. Also, exposure to high arterial shear stress at various exposure times reveals that platelet activation is sensitive to the high-level shear stress (>315 dyn/cm^2 at shear rate 10,500 s^{-1}) [6,47]. However, the mechanism of platelet activation caused by shear stresses is not fully understood [48]. Over the last four decades, two interesting theories have been proposed to uncover the precise role shear stress plays in platelet activation. One view holds that shear stress directly affects the activation and aggregation of platelets via vWF binding to platelet GPIbα receptor [5,49–51]. High shearing forces, acting on platelets, expose and activate the membrane GPIIb-IIIa complex. Thus, GPIbα and GPIIb-IIIa complex in the presence of vWF acting as the ligand will cause platelet aggregation. One potential explanation for the development of vWF binding sites after platelet activation is that GPIIb-IIIa receptors are hidden by other surface molecules in unstimulated platelets. When shear stresses deform platelets, their surface area increases enough to permit fibrinogen to reach GPIIb-IIIa complex. The signal transduction mechanisms mediating platelet aggregation by chemical stimuli and shear stress may be distinct [52]. Several

emerging mechanisms regarding shear-induced platelet mechanotransduction under supraphysiologic shear can be found in Refs. [53] and [54].

The other view of shear-induced platelet activation maintains that shear stress does not directly activate platelets. Platelets exposed to the shear stress are rather activated by the released agonists, principally ADP, stored in the intracellular granules, that results from the mechanical lysis of platelet and red cells caused by shear stress [55,56]. They argued that viscometry-based studies expose platelets and other blood cells to shear stress for seconds or, as quoted in most studies, minutes. This time duration appears to be 3 to 6 orders of magnitude longer than the time that blood flows through a high shear environment in heart valves, heart assists devices, and arterial stenoses, which is in the range of micro- to milliseconds. Based on experiments that exposed blood cells to shear stress ranging from 570 to 2550 dyn/cm^2 for time intervals from 7 to 700 ms, Wurzinger et al. found that the marker protein for platelet α-granule release (platelet activation), beta-thromboglobulin, behaved almost identically to the platelet lysis marker protein, cytoplasmic lactate dehydrogenase (LDH). Removing ADP from the tests via ADP-scavenging enzymes showed a mixture of discoid resting platelets intermingled with "ballooned" ruptured platelets with virtually no appearance of platelets in an activated state.

Apart from extensive studies of platelet activation caused by constant high shear stress, a few studies also investigated the roles of relatively low shear stress and time-varying shear stress. Sheriff et al. showed the sensitization phenomenon that platelet activation was more susceptible when platelets are exposed to subsequent low shear stress (1–10 dyn/cm^2) after brief exposure to initial high shear stress (e.g., 60 dyn/cm^2 for 40 s) [57]. Zhang et al. also showed the platelet aggregation is independent of platelet activation requiring low shear stress after a brief exposure (2.5 s) to the higher shear stress (100 dyn/cm^2) [45]. Goncalves et al. addressed the crucial role of temporal shear gradients (shear stress rate) in promoting platelet activation [58]. The study showed that cooperative signaling by platelet surface receptors is necessary for efficient shear activation of platelets. They suggested that vWF–GPIb interaction is inefficient at inducing platelet activation even when platelets are exposed to high wall shear stresses (60 dyn/cm^2). It implies the involvement of P2Y receptors in integrin mechanotransduction. Shear stress could likely contribute as direct signaling to the mechanotransduction of platelets, rendering activation of the $P2Y_{12}$ pathway by ADP [59]. In contrast, the study carried out by Schneider et al. shows platelets could be activated by GPIb binding to vWF without the $P2Y_{12}$ pathway [60]. In their investigation, the unfolding of the vWF fiber is induced by the shear reaches a critical shear rate, e.g., $\dot{\gamma}_{crit} \geq 5000\,s^{-1}$. Platelet is activated by binding to the vWF consequently. The shear stress conditions and exposure times discussed in the section are summarized in Table 1.

2.4 Blood Damage in Blood-Contacting Medical Devices. Blood-contacting medical devices are frequently used to treat patients suffering from various diseases and offer a life-saving option to prolong the survival of organ failure patients. For example, ventricular assist devices are increasingly used to support patients with heart failure [61,62], and extracorporeal membrane oxygenation systems are used to support patients suffering from lung and/or heart failure [63,64]. Despite the benefit of these therapies, BCMD-related complications remain a significant challenge for patient management and treatment outcomes, contributing to rising healthcare costs. In addition, blood damage associated with BCMDs becomes a principal limitation to the use of BCMDs. These devices can alter the structure of blood cells and proteins at the cellular and molecular levels, resulting in the dysfunction of blood cells and proteins.

Table 1 A summary of shear stress conditions and exposure times that activate platelets

Shear stress (shear rate)	Exposure time	References
60 dyn/cm^2	60–120 s	[46]
>315 dyn/cm^2	Various exposure times	[6] and [47]
570–2550 dyn/cm^2	7–700 ms	[55] and [56]
60 1–10 dyn/cm^2	40 s for 60 dyn/cm^2	[57]
100 dyn/cm^2	2.5 s	[45]
5000 s^{-1}	N/A	[60]

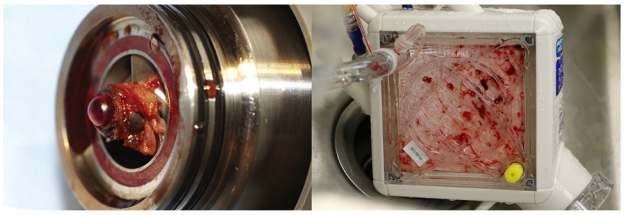

Fig. 3 Thrombus growth in medical devices. (*a*) HeartMate II left ventricular assist device [70] (Reproduced/Adapted with permission from Oxford Academic © 2011) and (*b*) Maquet Quadrox extracorporeal membrane oxygenation.

Hemolysis is one manifestation of mechanical damage to RBCs. Hemolysis in patients on BCMD support can lead to renal failure, anemia, and arrhythmias [26,65,66]. By contrast, adverse events pertinent to platelets can be more serious, raising more significant concerns. Platelet activation by BCMDs relates to more severe complications, such as thromboses and bleeding [67–69]. Figure 3 shows thrombus growth in a blood pump [70] and an oxygenator, respectively. Once a thrombus is detached, or a portion of the thrombus is broken off, it flows along with the bloodstream and blocks the smaller vessels downstream, creating a life-threatening condition known as thromboembolism. Also, platelet activation induced by the high mechanical shear stress would cause the exposure and shedding of platelet receptors that may affect platelet ligand binding to the agonist in the injury site. This shear-induced platelet dysfunction may be responsible for morbid bleeding, which is the most common postoperative complication after ventricular assist device implantation and the highest manifestation of disordered coagulation [71]. Although the inherent risk of platelet activation exposed to high shear stress is well known, yet little has been known about the precise mechanisms responsible for its initiation and progression. Therefore, it is difficult to achieve best practices to alleviate shear-induced platelet activation risk, which would further promote other undesirable outcomes such as thrombosis and bleeding.

3 Computational Modeling of Blood Flow

CFD has a broad definition that includes many numerical approaches to solve the mathematical models of fluid-like substances [72]. The conventional CFD technique often refers to the numerical method for solving Navier–Stokes (N–S) equations based on the continuum theory. Recent advances include the successful development of particle methods to study more details of blood cells in the blood flow [73,74]. Besides the conventional CFD, dissipative particle dynamics (DPD) and discrete element method (DEM) are briefly introduced in this section. Other newly developed methods, such as smoothed particle hydrodynamics and lattice Boltzmann method, for solving the blood flow can be found in Refs. [75] and [76].

3.1 Continuum Theory and N–S Equations. Based on the continuum theory, the N–S equations, using a set of partial differential equations (PDEs) to describe the viscous fluid substance's motion, are among the most popular modeling approaches for the

flow of fluids. The incompressible N–S equations are usually adequate to capture blood flow features. N–S equations are conventionally written in the Eulerian frame given as follows:

$$\rho\left[\partial \boldsymbol{u}/\partial t + (\boldsymbol{u}\cdot\nabla)\boldsymbol{u}\right] = \mu\nabla^2 u - \nabla p + \rho \boldsymbol{g} \tag{1}$$

where $\boldsymbol{u}$ is the velocity field of the fluid, t is the time, μ is the dynamic viscosity, and ρ is the density. p is the pressure. $\boldsymbol{g}$ is the external body force, such as gravity. The above N–S equations also imply the incompressible assumption, i.e., $u_{i,i} = 0$.

It is impossible to obtain analytical solutions via the N–S equations for fluid domains except for some simple geometries. Therefore, the N–S equations are often, in practice, solved by numerical methods based on discretized grid techniques. There are mainly three approaches, i.e., finite difference method [77], finite volume method (FVM) [78], and finite element method (FEM) [79–81]. All those methods convert PDEs into linear equations that can be solved by linear algebra in the matrix form. The finite difference method solves the N–S equations based on the original differential form of the PDEs (also known as strong form) that requires higher-order interpolation functions. The FVM and FEM, by contrast, require lower-order interpolation functions due to their integral forms of PDEs (also known as weak form). Although higher-order solutions are not easily obtained like FEM, the naturally encoded conservation law makes the FVM easier to code. It has thus been the most popular solver in engineering, well developed, and supported by commercial companies such as ANSYS/FLUENT and open source communities such as OPENFOAM [82].

3.2 Dissipative Particle Dynamics. Dissipative particle dynamics is relatively new in CFD. It uses a stochastic technique for simulating fluid dynamics [83] and can simulate complex fluid systems, such as fibers in viscous media and the dispersion of nanofluids, nanocomposites, and surfactants. Recently, it becomes a promising method to study the viscous flow and clot\thrombus formation in blood [73,84,85].

In the DPD approach, the fluid system is treated as a collection of particles governed by Newton's second law. The force acting on a particle is the sum of internal and external forces, i.e., $\boldsymbol{f}_i = \boldsymbol{f}_i^{\text{int}} + \boldsymbol{f}_i^{\text{ext}}$. The external forces ($\boldsymbol{f}_i^{\text{ext}}$) are given by gravity and other body forces. The total nonbond internal force ($\boldsymbol{f}_i^{\text{int}}$) acting the particle i is a sum over all particles j that lie within a certain cutoff distance

$$f_i^{\text{int}} = \sum_{j\neq i}\left(F_{ij}^c + F_{ij}^d + F_{ij}^r\right) \tag{2}$$

where F^c is conservative force, F^d is dissipative force, and F^r is random force. DPD allows for the simulation of many fluid properties, including its density, diffusivity, and source tension.

3.3 Discrete Element Method. The discrete element method can be viewed as a simpler version of smoothed particle hydrodynamics that uses particle groups to model a continuum object [86–88]. The equation of motion for each particle is governed by Newton's second law governs, and the interaction force is only concerned with adjacent particles that keep in touch directly. By summation of the forces and moments exerted by the neighboring particles in contact, the equations for linear and rotational motions of each particle are expressed as follows:

$$m_i\frac{d\boldsymbol{v_i}}{dt} = \boldsymbol{F}_i^F + \sum_{j=1}^{N} F_{ij} \tag{3}$$

$$I_i\frac{d\boldsymbol{\omega_i}}{dt} = \sum_{j=1}^{N} r_{ij}\times F_{ij} \tag{4}$$

where $\boldsymbol{v}$ is the translational velocity, m_i is the particle mass, and $\boldsymbol{F}^F$ is the external force such as gravity force and fluid-induced force. F_{ij} force is the contact force from neighboring particles j, and r_{ij} is the direct vector that connects the centers of particles i and j. I_i is the mass moment of the inertia. This method is intuitively employed to study problems with large numbers of discrete particles. Like DPD, in analyzing blood flow, DEM can either be used alone to model the blood flow or couples with CFD to simulate granular blood cells' movement.

4 Models of Shear-Induced Platelet Activation

In this section, several models for assessing the platelet activation under shear flow are discussed. They are generalized into two main categories: empirical and multiscale. Unlike empirical models, the multiscale platelet model built on the molecular scale does not need the empirical parameters from the experiment calibration.

4.1 Power-Law Model. The power-law model was initially proposed to associate blood damage/hemolysis with shear stress and exposure time from the experimental observation. The first power-law model, introduced by Giersiepen et al., attempted to relate the cytoplasm enzyme released by platelets to shear stress [13]. The concentration of LDH from platelet lysis is correlated to shear stress and exposure time

$$\text{LDH}(\%) = C\tau^{\alpha}t^{\beta} \tag{5}$$

where τ is the shear stress (Pa), and t is the exposure time (s). C, α, and β are model coefficients $(C,\alpha,\beta) = \left(3.31\times10^{-6}, 3.075, 0.77\right)$. The shear stress refers to the scalar shear stress (SSS) when incorporated power-law model into CFD analysis. It is originally introduced by Apel et al. [89] and Bludszuweit [90], but this formula gives an inconsistent SSS by a factor of $\sqrt{2}$ when flow field degenerates to the pure shear case, such as $\tau_{xy} = \tau_{yx} = \tau$ and other components vanish. To remove this inconsistency, a von Mises-like shear stress is used later to conventionally define SSS [91]

$$\tau = \left\{\frac{1}{6}\left[(\tau_{xx}-\tau_{yy})^2 + (\tau_{yy}-\tau_{zz})^2 + (\tau_{xx}-\tau_{zz})^2\right] + \tau_{xy}^2 + \tau_{yz}^2 + \tau_{xz}^2\right\}^{1/2} \tag{6}$$

where τ_{ij} is the shear stress tensor which is calculated by the product of shear rate ($\dot{\gamma}$) and viscosity (μ) such as $\tau_{ij} = \mu\dot{\gamma}_{ij}$. The shear rate is defined by the velocity gradient

$$\dot{\gamma}_{ij} = u_{i,j} + u_{j,i} \tag{7}$$

The coefficients in power-law model are conventionally obtained by fitting the experimentally measured data. An example of the data fitting of the power-law model for platelet activation is shown in Fig. 4(*a*). It is widely used to predict blood damage [92–94]. Although agonists such as ADP released from platelet lysis can be viewed as a sign of platelet activation, LDH production is not directly relative to the platelet activation state (PAS). Following the same formula, Sheriff et al. used a modified prothrombinase assay, which generated thrombin, to quantify PAS as an index for calculating the rate of thrombin generation [95]

$$\text{PAS} = C\tau^{\alpha}t^{\beta} \tag{8}$$

They fitted the coefficients as $(C,\alpha,\beta) = \left(1.47\times10^{-6}, 1.04, 1.30\right)$, where the unit of shear stress is dyn/cm^2 and exposure time in s. Based on the p-selectin expression, Ding et al. fitted the power-law relationship of platelet activation $(C,\alpha,\beta) = \left(4.08\times10^{-5}, 1.56, 0.8\right)$, the unit of shear is Pa, and exposure time in s [16].

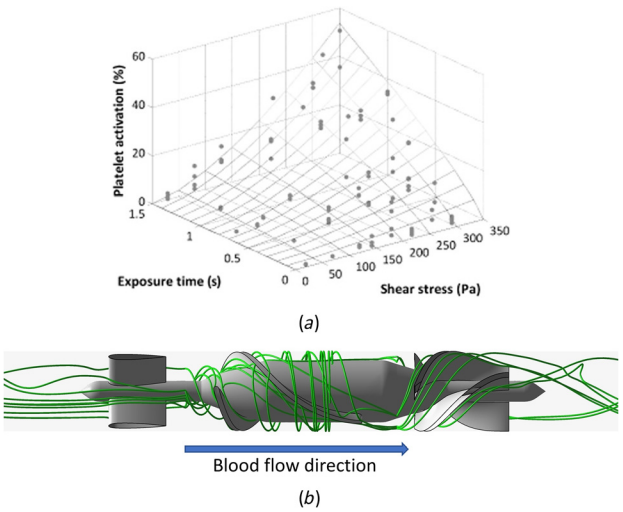

Fig. 4 The example of (*a*) data fitting of the power-law model [16] (Reproduced/Adapted with permission from Wiley © 2015) and (*b*) pathlines (green lines) from the CFD simulation of a HeartMate II.

The power-law model can be implemented in CFD modeling of BCMDs for analysis of shear-induced platelet activation. There are two approaches, i.e., Eulerian and Lagrangian approaches, to estimate shear-induced blood damage (hemolysis, platelet activation) in a given fluid domain. The Eulerian approach integrates on the spatial domain. For example, Garon and Farinas in Ref. [96] proposed to use the following formula to transform the power-law relation:

$$D = \left[\frac{1}{Q}\int_V C^{1/\alpha}\tau^{\beta/\alpha}dV\right]^{\alpha} \tag{9}$$

where D is the blood damage index (hemolysis or platelet activation level). Q is the flow rate, and V is the volume. The Lagrangian approach integrates the blood damage based on the stress history along tracer particle streaklines or pathlines. An example of pathlines from the CFD simulation of a HeartMate II is displayed in Fig. 4(*b*). The discrete and infinitesimal forms of the power-law model are used as follows:

$$D = \sum C\tau_i^{\beta}\Delta t_i^{\alpha} \tag{10}$$

$$dD = C\tau^{\beta}dt^{\alpha} \tag{11}$$

where Δt is the time interval across an element. Grigioni et al. showed that the total damage calculated by the above infinitesimal form cannot reproduce the power-law concept under constant shear stress [94,97]. Some authors suggested the temporal derivative form of discrete and infinitesimal forms to avoid this inconsistency [97]

$$D = \sum C\alpha\tau_i^{\beta}t_i^{\alpha-1}\Delta t_i \tag{12}$$

$$dD = C\alpha\tau^{\beta}t^{\alpha-1}dt \tag{13}$$

The overall blood damage state through pathlines through a BCMD can then be integrated from particles releasing from inlet to outlet. Although the temporal derivative does reproduce the total damage given by the power-law equation, it does not depend on the damage history.

4.2 Linear Model. The linear model is a special case of the power-law model where all parameters equal to one, i.e., $(C, \alpha, \beta) = (1, 1, 1)$. It is one of the most popular alternatives due to its simplest form gives as [17,85,98–100]. The PAS is expressed as

$$\text{PAS} = \tau \times t \tag{14}$$

Similar to the power-law model, the sum of the shear stress along a single platelet path in the Lagrangian form determines the PAS. The discrete expression of tracking a platelet gives

$$\text{PAS} = \sum \tau \times \Delta t \tag{15}$$

The integral form calculates the shear stress accumulation of a platelet particle as it is released from the inlet, such as

$$\text{PAS} = \int \tau dt \tag{16}$$

4.3 Three-Term Model. The three-term model proposed by Soares et al. [101] incorporates the sensitization phenomenon. The PAS in the three-term model is an implicit expression considering sensitization response, shear stress accumulation, and shear stress rate [101–104]

$$\frac{d\text{PAS}(t)}{dt} = K_0\left[\text{PAS}, \tau^{(t)}(s)\right](1 - \text{PAS}) \tag{17}$$

Platelet activation level can vary from zero (no activation/damage) to one (full activation/damage). K_0 is the initial rate of the stress-induced platelet activation when PAS = 0. The platelet activation rate at high PAS levels also follows a logistic saturation as PAS $\to$ 1, $d\text{PAS}/dt \to 0$, which is interpreted as when platelets reach full activation asymptotically, their activation rate vanishes. The three-term model determines stress-induced platelet activation by three different and distinctive additive efforts of the general form

$$K_0\left[\text{PAS}, \tau^{(t)}(s)\right] = S(\text{PAS}, H_\tau) + F(\text{PAS}, \tau) + G(\text{PAS}, \dot{\tau}) \tag{18}$$

where H_τ represents the history of damage that calculates the linear stress accumulation until current time t. As same as Eq. (16), it defines as

$$H_\tau = \int_0^t \tau(s)ds \tag{19}$$

S is the sensitization response to the stress accumulation

$$S(\text{PAS}(t), H_\tau) = S_r \cdot \text{PAS}(t) \cdot H_\tau \tag{20}$$

F is the stress level contribution like the power-law model, and G is the stress rate dependence. They both are nonlinear terms defined as follows:

$$F(\text{PAS}(t), \tau) = C^{\frac{1}{\beta}} \cdot \beta \cdot \text{PAS}(t)^{\frac{\beta-1}{\beta}}\tau^{\frac{\alpha}{\beta}} \tag{21}$$

$$G(\text{PAS}(t), \dot{\tau}) = C_r^{\frac{1}{\delta}} \cdot \text{PAS}(t)^{\frac{\delta-1}{\delta}}|\dot{\tau}|^{\frac{\gamma}{\delta}} \tag{22}$$

where C, S_r, β, α, C_r, δ, and γ are constants.

4.4 Cumulative Model. The cumulative model is initially developed to evaluate hemolysis. A damage accumulation model is given as

$$\frac{dD(t)}{dt} = \dot{D}_0 + F(D, \tau) + \hat{F}(\dot{\tau}) \tag{23}$$

where $\dot{D}_0$ is the constant activation/damage rate, $F(D,\tau)$ is the stress-dependent part, and $\hat{F}(\dot{\tau})$ is the stress rate-dependent contribution. Alemu and Bluestein [20] quantified the platelet activation based on the theory of damage previously developed for RBC damage by Yeleswarapu et al. [105], defined as follows:

$$\dot{A}(t) = \left[\frac{\tau(t)}{\tau_0}\right]^r \left[\frac{1}{(1-A(t))^k}\right] \tag{24}$$

where $A(t)$ is the cumulative damage due to the shear stress at time t, which can vary from zero (no activation/damage) to one (full activation/damage). r and k are constants with the value of 5 and -1, respectively. This implicit cumulative model is similar to the three-term model.

The explicit Lagrangian-based cumulative model has been modified based on the measurement of thrombin generation rate under dynamic loading conditions. It can account for load history sustained by platelets exposed to time-dependent stress levels. In detail, the activation state of a platelet is expressed as the integral sum of infinitesimal [21]

$$\mathrm{PAS} = \int_{t^{\mathrm{start}}}^{t} \mathrm{Ca}\left[\int_{t^{\mathrm{start}}}^{\phi} \tau(\xi)^{b/a} d\xi + \frac{\mathrm{PAS}(t^{\mathrm{start}})^{1/a}}{C}\right]^{a-1} \tau(\phi)^{b/a} d\phi \tag{25}$$

$\mathrm{PAS}(t^{\mathrm{start}})$ is the value of platelet activation at the starting time of observation t^{start}, and $a = 1.3198$, $b = 0.6256$, and $C = 10^{-5}$ are the constants of the model. A prediction of the platelet activation is obtained by the calculation of the average value of PAS.

Anand et al. proposed another approach to quantify platelet exposure to excessive stress leading to its activation in complex flows [18,106,107]. It considers the platelet activation function A as an integral over the platelet stressing history

$$A(t) = A(t_0) + \frac{1}{A_0}\int_{t_0}^{t} \exp\left[k\left(\frac{\tau(\xi)}{\tau_c} - 1\right)\right] H(\tau(\xi) - \tau_c) d\xi \tag{26}$$

where H is the Heaviside function to assure that only supracritical stresses are taken into consideration, i.e., contributing to platelet activation and defines as

$$H(\tau - \tau_c) = \begin{cases} 1 & \text{if} \quad \tau \geq \tau_c \\ 0 & \text{if} \quad \tau < \tau_c \end{cases} \tag{27}$$

This Lagrangian model assumes that the platelets are activated after being exposed to high shear stress along pathlines for some time. To account for the immediate platelet activation, Bodnár proposed the Eulerian form [19]

$$\frac{\partial A}{\partial t} + u\nabla A = C_0 \exp\left[k\left(\frac{\tau(x,t)}{\tau_c} - 1\right)\right] H(\tau(x,t) - \tau_c) \tag{28}$$

The expression is close to the form of convection–diffusion–reaction equations in Fogelson's model of clot formation [108,109].

4.5 Threshold Model. Unlike the above models that relate the level of platelet activation to the shear stress and exposure time, the threshold model determines the platelet activation as zero or one event by comparing the exposed shear stress to a critical value. The threshold shear model proposed by Chesnutt and co-workers assumes the platelet activated if it experiences shear stress above a critical shear stress τ_{crit} defined as [110–112]

$$\tau_{\mathrm{crit}} = f|\tau_0| \tag{29}$$

where f is a scaling factor, and τ_0 is the shear stress in a straight vessel with the same mean fluid velocity and vessel diameter as the actual vessel. This shear stress can also be an average value in the specific region; for example, $\bar{\tau} = 1/V \int \tau dV$ [113]. The PAS is defined as a one or zero event, that is

$$\mathrm{PAS} = \begin{cases} 1 & \text{if} \quad \tau \geq \tau_{\mathrm{crit}} \\ 0 & \text{if} \quad \tau < \tau_{\mathrm{crit}} \end{cases} \tag{30}$$

An alternative approach is based on the critical shear rate ($\dot{\tau}_{\mathrm{crit}} = f|\dot{\tau}_0|$) to ignore the effect of viscosity [23,114]. One can also determine the activation of platelet by comparing the stress accumulation (H_τ) in Eq. (19) with a critical shear history H_{crit} [115]

$$\mathrm{PAS} = \begin{cases} 1 & \text{if} \quad H_\tau \geq H_{\mathrm{crit}} \\ 0 & \text{if} \quad H_\tau < H_{\mathrm{crit}} \end{cases} \tag{31}$$

Some nonlinear models would add an exponential index to the shear term, $H_\tau = \int_0^t \tau^\alpha(s) ds$, for example, $\alpha = 2.3$ in Refs. [116] and [117]. The threshold model is also adopted in the power-law model only to consider platelets that have experienced high shear stress above a threshold level [118].

4.6 Multiscale Platelet Model. Although the above models are classified into different categories, they are, in essence, all variants of the initial power-law models that depend on the empirical parameters obtained by fitting experimental data. Zhang et al. constructed a platelet model based on the coarse-grained molecular dynamics (CGMD) [24,25,119], as shown in Fig. 5. A reduced CGMD potential is adopted for the elastic membrane and filamentous core

$$V_{\mathrm{CGMD}}(r) = \sum_{\mathrm{bonds}} k_b (r - r_0)^2 + \sum_{L\text{–}J} 4\varepsilon_{ij}\left[\left(\frac{\sigma_{ij}}{r}\right)^{12} - \left(\frac{\sigma_{ij}}{r}\right)^{6}\right] \tag{32}$$

The first term describes the membrane's deformability, and the second term deals with the interaction between the membrane and intracellular particles. The molecular dynamics potential without an electrostatic term is employed to build the actin-based filament, that is

$$\begin{aligned} V_{\mathrm{MD}}(r) = &\sum_{\mathrm{bonds}} k_b (r - r_0)^2 + \sum_{\mathrm{angles}} k_\theta (\theta - \theta_0)^2 \\ &+ \sum_{\mathrm{torsion}} k_\phi [1 + \cos(n\phi - \delta)] \\ &+ \sum_{L\text{–}J} 4\varepsilon_{ij}\left[\left(\frac{\sigma_{ij}}{r}\right)^{12} - \left(\frac{\sigma_{ij}}{r}\right)^{6}\right] \end{aligned} \tag{33}$$

where k_b, k_θ, and k_ϕ are force constants. r and θ are the distance and angle between particles, and r_0 and θ_0 are the distance and angle at the equilibrium state. ϕ is the torsional angle. n is the rotor symmetric, and δ is the phase. ε_{ij} is the depth of the Lennard-Jones potential, and σ_{ij} is the finite distance.

The Morse potential is employed for the cytoplasm describing a pairwise nonbonded interaction for viscous flows has the following formulation:

$$V_{\mathrm{Morse}}(r) = 4\varepsilon\left[e^{\alpha\left(1-\frac{r}{R}\right)} - 2e^{\frac{\alpha}{2}\left(1-\frac{r}{R}\right)}\right] \tag{34}$$

where R is the distance of minimum energy ε. α is a parameter that measures the curvature of the potential around R. This CGMD model of the platelet interacts with the DPD flow. The continuously deformation-induced stresses cause the platelet's instantaneous deformation, indicating the activation level [24].

5 Numerical Implementation and Applications

Platelet activation was often negligible and treated as a minor component of blood damage in the past. It has recently been

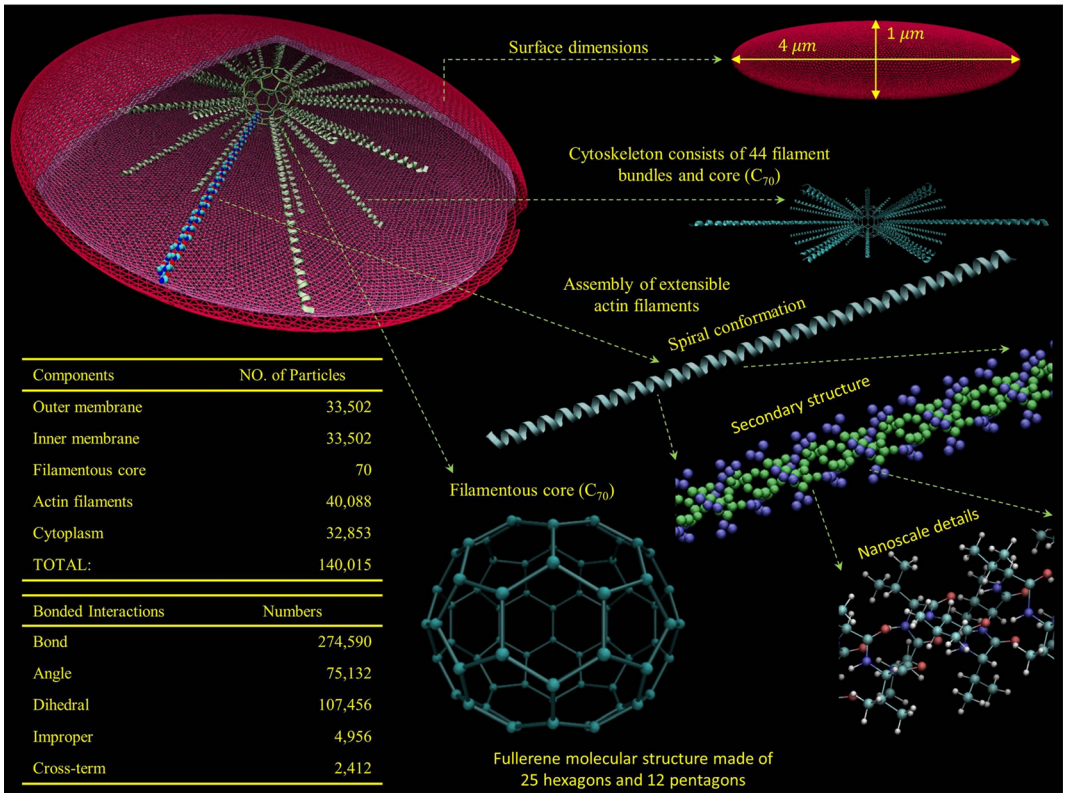

Fig. 5 The multiscale model of platelet based on the CGMD featuring the molecular characteristics of the platelet [25] (Reproduced/Adapted with permission from Elsevier © 2017)

recognized as an essential factor in hemostatic dysfunction and became an important indicator to estimate the impact of shear stress on the blood. A few simulations on clot formulation also incorporated the shear-induced platelet activation models to mimic the primary hemostasis initiated by the activated platelets. To understand the mechanism of how shear stress induces the platelet activation, some attempted to study the dynamic response of platelet and vWF to the shear stress based on the construction of their detailed molecular structures.

5.1 Blood Damage Evaluation. The investigation of the shear-induced platelet activation is often viewed as a part of blood damage analysis [105]. Numerous studies have been performed to evaluate blood damage caused by biomedical devices or specific blood domains [91,94,120,121]. However, the focus of most of these studies was on hemolysis. The first step in the analysis is to obtain the fluid fields constrained in various geometries by employing the conventional CFD techniques. The blood damage index is then estimated mainly through implementing the power-law models, either based on the Eulerian or the Lagrangian approaches. The blood damage accumulation model is another popular method to evaluate blood damage [97,122]. More detailed reviews of the blood damage due to the shear stress are available in Refs. [11] and [93]. The computational flow-induced blood damage analysis is a valuable tool for the design optimization of a new medical device.

5.2 Platelet Activation Potential. Similar to the hemolysis evaluation, the first step for evaluating platelet activation is to solve the fluid field using CFD techniques, and then the platelet activation potential is estimated by incorporating various models for shear-induced platelet activation. A few recent works on the numerical evaluation of the shear-induced platelet activation are briefly discussed here. Alemu and Bluestein investigated the platelet activation and damage accumulation caused by mechanical heart valves using linear power-law and cumulative models [20]. The simulation was conducted in a three-dimensional complex geometry using unsteady Reynolds-averaged N–S formulation with non-Newtonian blood properties. Hansen et al. studied the platelet activation in the abdominal aortic aneurysms using a power-law model [123]. Incorporating the power-law model, Fuchs et al. studied the flow-induced platelet activation in the circuit components of the extracorporeal membrane oxygenation [15]. A main shortcoming in the accumulation stress effect based on the power-law model is that it does not distinguish the outcomes between low-stress over a longer time or high-stress over a shorter time. Hedayat et al. evaluated the platelet activation potential related to bileaflet mechanical heart valves using three models, i.e., linear model, three-term model, and cumulative model [102,103]. Although different activation models gave different values of platelet activation levels, they showed a consistent trend. de Oliveira et al. assessed the platelet activation caused by the dialysis catheters on the right atrium using the shear stress threshold model [113]. The contour of shear stress could efficiently visualize the platelet activation level, but the stress history on the platelet was ignored.

5.3 Clot Formation. In recent years, numerical simulation of clot formulation or thrombus growth has gained popularity. However, most of the numerical models were focused on the fibrin-enhanced thrombus, using a set of convection–diffusion–reaction equations to emulate the biochemical process of clot formation. A brief review of the computational models on clot formation can be found in Ref. [31].

The flow-induced platelet activation is crucial in medical devices since it can irreversibly initiate the coagulation cascade leading to life-threatening clot formation in patients. There are two approaches for flow-induced clot formation, i.e., the continuum approach and the discrete particle approach. Figure 6 shows a schematic comparison between these two methods for clot simulation. By implementing the Eulerian cumulative model in the

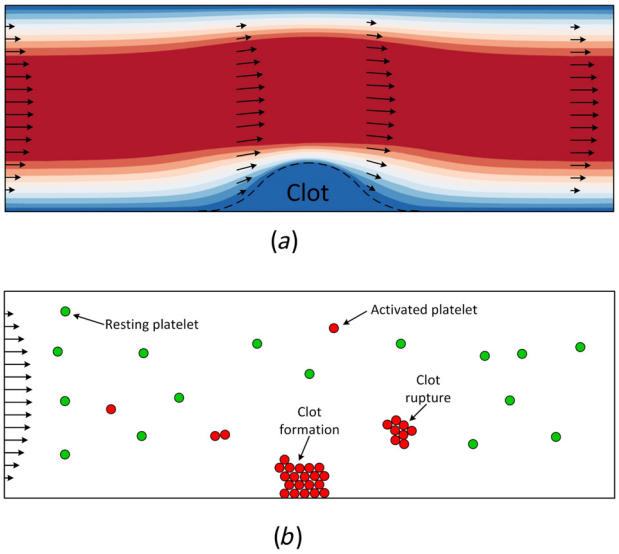

Fig. 6 The comparison of (*a*) continuum and (*b*) particle-based approaches for clot formation

conventional CFD analysis, Wu et al. conducted a clot formation simulation enhanced by the shear-mediated platelet activation [22]. This model can predict clot formation in medical devices on the macroscale. The platelet activation level is obtained by solving the differential equation, such as in Eq. (28); no actual platelet is modeled.

The discrete model, e.g., DPD and DEM, uses particles or beads to represent different cells in the blood. The clot formation is modeled as the aggregation of the particles. For example, thrombus formation in microvessels is simulated through DEM, in which platelet is determined as activated when it experiences shear stress higher than the critical value [110]. Wang et al. emulated clot formation aggregated by particles based on the DPD model with the power-law model determining whether a platelet is activated or not [74]. The particle-represented blood models are flexible to model complex blood components, such as non-Newtonian and compressible fluid. They are more intuitive and powerful to feature different blood cells, but the expensive computational cost limits its usage on the macroscale.

5.4 Mechanistic Study. To better understand the shear-induced platelet activation mechanism, some research groups recently attempted to build the structures of platelet or vWF with more details. A multiscale model of the platelet was built based on the CGMD [25]. The deformation of a single platelet was obtained, coupling with the DPD blood, to indicate platelet activation [24]. Zlobina and co-workers simulated the unfolding of the vWF in the blood flow that causes the dynamic conformational changes of platelet, resulting in its activation [115,124]. These approaches are relatively new, but the physical-based models are more promising to reveal the mechanism of how shear stress induces platelet activation.

6 Discussion

Overall, computational modeling for the flow/shear-induced platelet activation has shown a gradual but steady advance over the years. Although many models have been proposed and developed as detailed in Sec. 4, most of them are, in essence, empirical approaches modified from the original power-law model fitting to the experimental data. Many studies showed the overestimated platelet activation using these empirical models. Also, they cannot provide universal approaches for different cases under different fluid flow conditions. By contrast, the multiscale model, building a detailed architecture of a single platelet, does not require the parameters calibrated by experiments. It is a distinct approach that evaluates platelet activation by measuring its deformation in the bloodstream. Yet, adopting such a model to simulate platelet activation in a complex blood flow at a larger scale can be numerically too expensive to achieve.

The recent trend in the studies of shear-induced platelet activation saw the shift from the early evaluation of hemolysis to the risk assessment of platelet activation potential and clot formation simulation. The particle methods such as DPD and DEM and emerging techniques such as multiscale modeling are promising and increasingly used to replace the continuum method. However, continuum methods are still suitable and powerful for evaluating platelet activation potentials and predicting thrombus formation, especially for large-scale cases.

The continuum models of blood are valuable to understand the fundamental behavior of the blood under mechanical shear stress. A single RBC is modeled as a spring network of the biconvex membrane in recent researches on hemolysis [66,125–127]. Measuring the pore radius due to the deformation of RBC's membrane, hemolysis can be explained by the hemoglobin diffusion/leakage [26]. Compared to the stable form of the RBC, the cellular structure and topology of a platelet are more complicated. The biggest challenge is the drastic morphological change upon platelet activation, flat discoid shape at resting state changes to the spiny sphere at activated state.

Recent biological experiments have revealed that the platelet structure comprises a MB, consisting of several microtubules and a cortical membrane [128,129]. Through the observation from the immunofluorescent images, MB coils when platelet is activated. The platelet's shape change is due to the force balance between the MB and membrane [130,131]. Such a hypothesis may provide an insightful interpretation of platelets' morphological change that can be employed to study shear-induced platelet activation quantitatively. Some emerging mechanisms, including mechanodestruction, mechano-activation, and mechanotransduction, may offer a potential explanation on how shear stress modulates the material properties of the platelet, such as overall stiffness, membrane fluidity, or platelet-activating biochemical signals, that enhance the platelet activation [53,54,132]. However, platelet activation also involves complex biological and chemical reactions, making it difficult to fully understand the precise mechanism.

The future challenge of the numerical models for the shear-induced platelet activation is to develop a robust and computationally efficient platform capable of multiscale tasks, from tracking the platelet morphological change as an index of its activation to tackling the clot formation initiated by platelet activation. Although much has been done so far from the experimental side, it is still unclear how the shear stress is transformed as a biochemical signal that activates the platelet. The future shear-induced platelet activation models would enormously benefit from having that knowledge which, unfortunately, is not yet available.

7 Conclusion

This paper has summarized the recent developments in the computational models of shear stress-induced platelet activation. We discussed several empirical models like the power-law model, linear model, three-term model, cumulative model, and threshold model coupled with conventional CFD to estimate the level of shear-induced platelet activation. A newly multiscale platelet model becomes a promising method to capture the dynamic deformation, a sign of activation, of a single platelet in the complex fluid. The strengths and weaknesses of the existing methods are critically analyzed. The trend and the future direction lead to the models that can feature platelet morphological change upon its activation and a feasible algorithm for the clot formation initiated by the shear-induced platelet activation.

Acknowledgment

The author(s) disclosed receipt of the following financial support for the research, authorship, and/or publication of this article:

This work was funded by National Institutes of Health (Grant Nos. R01HL118372, R01HL124170, R01HL131750, and R01HL141817).

Funding Data

- National Institutes of Health (Grant Nos. R01HL118372, R01HL124170, R01HL131750, and R01HL141817; Funder ID: 10.13039/100000002).

Conflict of Interest

The author(s) declared no potential conflicts of interest with respect to the research, authorship, and/or publication of this article.

References

[1] Minors, D. S., 2007, "Haemostasis, Blood Platelets and Coagulation," Anaesth. Intensive Care Med., **8**(5), pp. 214–216.
[2] Engelmann, B., and Massberg, S., 2013, "Thrombosis as an Intravascular Effector of Innate Immunity," Nat. Rev. Immunol., **13**(1), pp. 34–45.
[3] Clemetson, K. J., 2012, "Platelets and Primary Haemostasis," Thromb. Res., **129**(3), pp. 220–224.
[4] O'Brien, J., 1990, "Shear-Induced Platelet Aggregation," Lancet, **335**(8691), pp. 711–713.
[5] Hellums, J., Peterson, D., Stathopoulos, N., Moake, J., and Giorgio, T., 1987, "Studies on the Mechanisms of Shear-Induced Platelet Activation," *Cerebral Ischemia and Hemorheology*, Springer, Berlin, pp. 80–89.
[6] Holme, P. A., Ørvim, U., Hamers, M. J., Solum, N. O., Brosstad, F. R., Barstad, R. M., and Sakariassen, K. S., 1997, "Shear-Induced Platelet Activation and Platelet Microparticle Formation at Blood Flow Conditions as in Arteries With a Severe Stenosis," Arterioscler., Thromb., Vasc. Biol., **17**(4), pp. 646–653.
[7] Thamsen, B., Blümel, B., Schaller, J., Paschereit, C. O., Affeld, K., Goubergrits, L., and Kertzscher, U., 2015, "Numerical Analysis of Blood Damage Potential of the HeartMate II and HeartWare HVAD Rotary Blood Pumps," Artif. Organs, **39**(8), pp. 651–659.
[8] Fraser, K. H., Zhang, T., Taskin, M. E., Griffith, B. P., and Wu, Z. J., 2012, "A Quantitative Comparison of Mechanical Blood Damage Parameters in Rotary Ventricular Assist Devices: Shear Stress, Exposure Time and Hemolysis Index," ASME J. Biomech. Eng., **134**(8), p. 081002.
[9] Burgreen, G. W., Antaki, J. F., Wu, Z., and Holmes, A. J., 2001, "Computational Fluid Dynamics as a Development Tool for Rotary Blood Pumps," Artif. Organs, **25**(5), pp. 336–340.
[10] Song, X., Throckmorton, A. L., Wood, H. G., Antaki, J. F., and Olsen, D. B., 2003, "Computational Fluid Dynamics Prediction of Blood Damage in a Centrifugal Pump," Artif. Organs, **27**(10), pp. 938–941.
[11] Yu, H., Engel, S., Janiga, G., and Thévenin, D., 2017, "A Review of Hemolysis Prediction Models for Computational Fluid Dynamics," Artif. Organs, **41**(7), pp. 603–621.
[12] Taskin, M. E., Fraser, K. H., Zhang, T., Wu, C., Griffith, B. P., and Wu, Z. J., 2012, "Evaluation of Eulerian and Lagrangian Models for Hemolysis Estimation," ASAIO J., **58**(4), pp. 363–372.
[13] Giersiepen, M., Wurzinger, L., Opitz, R., and Reul, H., 1990, "Estimation of Shear Stress-Related Blood Damage in Heart Valve Prostheses—In Vitro Comparison of 25 Aortic Valves," Int. J. Artif. Organs, **13**(5), pp. 300–306.
[14] Owen, D. G., de Oliveira, D. C., Qian, S., Green, N. C., Shepherd, D. E., and Espino, D. M., 2020, "Impact of Side-Hole Geometry on the Performance of Hemodialysis Catheter Tips: A Computational Fluid Dynamics Assessment," PLoS One, **15**(8), p. e0236946.
[15] Fuchs, G., Berg, N., Broman, L. M., and Wittberg, L. P., 2018, "Flow-Induced Platelet Activation in Components of the Extracorporeal Membrane Oxygenation Circuit," Sci. Rep., **8**(1), p. 13985.
[16] Ding, J., Chen, Z., Niu, S., Zhang, J., Mondal, N. K., Griffith, B. P., and Wu, Z. J., 2015, "Quantification of Shear-Induced Platelet Activation: High Shear Stresses for Short Exposure Time," Artif. Organs, **39**(7), pp. 576–583.
[17] Bluestein, D., Niu, L., Schoephoerster, R. T., and Dewanjee, M. K., 1997, "Fluid Mechanics of Arterial Stenosis: Relationship to the Development of Mural Thrombus," Ann. Biomed. Eng., **25**(2), pp. 344–356.
[18] Anand, M., and Rajagopal, K. R., 2002, "A Mathematical Model to Describe the Change in the Constitutive Character of Blood Due to Platelet Activation," C. R. Mec., **330**(8), pp. 557–562.
[19] Bodnár, T., 2014, "On the Eulerian Formulation of a Stress Induced Platelet Activation Function," Math. Biosci., **257**, pp. 91–95.
[20] Alemu, Y., and Bluestein, D., 2007, "Flow-Induced Platelet Activation and Damage Accumulation in a Mechanical Heart Valve: Numerical Studies," Artif. Organs, **31**(9), pp. 677–688.
[21] Nobili, M., Sheriff, J., Morbiducci, U., Redaelli, A., and Bluestein, D., 2008, "Platelet Activation Due to Hemodynamic Shear Stresses: Damage Accumulation Model and Comparison to In Vitro Measurements," ASAIO J., **54**(1), pp. 64–72.
[22] Wu, W.-T., Zhussupbekov, M., Aubry, N., Antaki, J. F., and Massoudi, M., 2020, "Simulation of Thrombosis in a Stenotic Microchannel: The Effects of vWF-Enhanced Shear Activation of Platelets," Int. J. Eng. Sci., **147**, p. 103206.
[23] Chesnutt, J. K., and Han, H.-C., 2013, "Platelet Size and Density Affect Shear-Induced Thrombus Formation in Tortuous Arterioles," Phys. Biol., **10**(5), p. 056003.
[24] Zhang, P., Sheriff, J., Einav, S., Slepian, M. J., Deng, Y., and Bluestein, D., 2021, "A Predictive Multiscale Model for Simulating Flow-Induced Platelet Activation: Correlating In Silico Results With In Vitro Results," J. Biomech., **117**, p. 110275.
[25] Zhang, P., Zhang, L., Slepian, M. J., Deng, Y., and Bluestein, D., 2017, "A Multiscale Biomechanical Model of Platelets: Correlating With In-Vitro Results," J. Biomech., **50**, pp. 26–33.
[26] Nikfar, M., Razizadeh, M., Zhang, J., Paul, R., Wu, Z. J., and Liu, Y., 2020, "Prediction of Mechanical Hemolysis in Medical Devices Via a Lagrangian Strain-Based Multiscale Model," Artif. Organs, **44**(8), pp. E348–E368.
[27] Levin, J., 2019, "The Evolution of Mammalian Platelets," *Platelets*, Elsevier, Academic Press, Cambridge, MA, pp. 1–23.
[28] Quinn, M., Fitzgerald, D., and Cox, D., 2007, *Platelet Function: Assessment, Diagnosis, and Treatment*, Springer Science & Business Media, Berlin.
[29] Cito, S., Mazzeo, M. D., and Badimon, L., 2013, "A Review of Macroscopic Thrombus Modeling Methods," Thromb. Res., **131**(2), pp. 116–124.
[30] Adams, R. L., and Bird, R. J., 2009, "Coagulation Cascade and Therapeutics Update: Relevance to Nephrology. Part 1: Overview of Coagulation, Thrombophilias and History of Anticoagulants," Nephrology, **14**(5), pp. 462–470.
[31] Yesudasan, S., and Averett, R. D., 2019, "Recent Advances in Computational Modeling of Fibrin Clot Formation: A Review," Comput. Biol. Chem., **83**, p. 107148.
[32] White, J. G., and Rao, G., 1998, "Microtubule Coils Versus the Surface Membrane Cytoskeleton in Maintenance and Restoration of Platelet Discoid Shape," Am. J. Pathol., **152**(2), pp. 597–609.
[33] Kunert, S., Meyer, I., Fleischhauer, S., Wannack, M., Fiedler, J., Shivdasani, R. A., and Schulze, H., 2009, "The Microtubule Modulator RanBP10 Plays a Critical Role in Regulation of Platelet Discoid Shape and Degranulation," Blood, **114**(27), pp. 5532–5540.
[34] White, J. G., and Estensen, R. D., 1972, "Degranulation of Discoid Platelets," Am. J. Pathol., **68**(2), pp. 289–302.
[35] Italiano, J. E., Jr., Bergmeier, W., Tiwari, S., Falet, H., Hartwig, J. H., Hoffmeister, K. M., André, P., Wagner, D. D., and Shivdasani, R. A., 2003, "Mechanisms and Implications of Platelet Discoid Shape," Blood, **101**(12), pp. 4789–4796.
[36] Bearer, E., Prakash, J., and Li, Z., 2002, "Actin Dynamics in Platelets," Int. Rev. Cytol., **217**, pp. 137–182.
[37] Allen, R. D., Zacharski, L. R., Widirstky, S. T., Rosenstein, R., Zaitlin, L. M., and Burgess, D. R., 1979, "Transformation and Motility of Human Platelets: Details of the Shape Change and Release Reaction Observed by Optical and Electron Microscopy," J. Cell Biol., **83**(1), pp. 126–142.
[38] Shin, E.-K., Park, H., Noh, J.-Y., Lim, K.-M., and Chung, J.-H., 2017, "Platelet Shape Changes and Cytoskeleton Dynamics as Novel Therapeutic Targets for Anti-Thrombotic Drugs," Biomol. Ther., **25**(3), pp. 223–230.
[39] White, J. G., 2005, "Platelets Are Covercytes, Not Phagocytes: Uptake of Bacteria Involves Channels of the Open Canalicular System," Platelets, **16**(2), pp. 121–131.
[40] Ramadori, P., Klag, T., Malek, N. P., and Heikenwalder, M., 2019, "Platelets in Chronic Liver Disease, From Bench to Bedside," JHEP Rep., **1**(6), pp. 448–459.
[41] Jesty, J., Yin, W., Perrotta, P., and Bluestein, D., 2003, "Platelet Activation in a Circulating Flow Loop: Combined Effects of Shear Stress and Exposure Time," Platelets, **14**(3), pp. 143–149.
[42] Hellums, J. D., 1994, "1993 Whitaker Lecture: Biorheology in Thrombosis Research," Ann. Biomed. Eng., **22**(5), pp. 445–455.
[43] Ramstack, J., Zuckerman, L., and Mockros, L., 1979, "Shear-Induced Activation of Platelets," J. Biomech., **12**(2), pp. 113–125.
[44] Reinthaler, M., Johansson, J. B., Braune, S., Al-Hindwan, H. S. A., Lendlein, A., and Jung, F., 2019, "Shear-Induced Platelet Adherence and Activation in an In-Vitro Dynamic Multiwell-Plate System," Clin. Hemorheol. Microcirc., **71**(2), pp. 183–191.
[45] Zhang, J.-N., Bergeron, A. L., Yu, Q., Sun, C., McIntire, L. V., López, J. A., and Dong, J.-F., 2002, "Platelet Aggregation and Activation Under Complex Patterns of Shear Stress," Thromb. Haemostasis, **88**(11), pp. 817–821.
[46] Giorgio, T., and Hellums, J., 1988, "A Cone and Plate Viscometer for the Continuous Measurement of Blood Platelet Activation," Biorheology, **25**(4), pp. 605–624.
[47] Ruggeri, Z. M., 2002, "Platelets in Atherothrombosis," Nat. Med., **8**(11), pp. 1227–1234.
[48] Hansen, C. E., Qiu, Y., McCarty, O. J., and Lam, W. A., 2018, "Platelet Mechanotransduction," Annu. Rev. Biomed. Eng., **20**(1), pp. 253–275.
[49] Konstantopoulos, K., Wu, K., Udden, M., Banez, E., Shattil, S., and Hellums, J., 1995, "Flow Cytometric Studies of Platelet Responses to Shear Stress in Whole Blood," Biorheology, **32**(1), pp. 73–93.
[50] McCrary, J. K., Nolasco, L. H., Hellums, J. D., Kroll, M. H., Turner, N. A., and Moake, J. L., 1995, "Direct Demonstration of Radiolabeled von Willebrand Factor Binding to Platelet Glycoprotein Ib and IIb-IIIa in the Presence of Shear Stress," Ann. Biomed. Eng., **23**(6), pp. 787–793.
[51] Reininger, A. J., Heijnen, H. F., Schumann, H., Specht, H. M., Schramm, W., and Ruggeri, Z. M., 2006, "Mechanism of Platelet Adhesion to von

Willebrand Factor and Microparticle Formation Under High Shear Stress," Blood, **107**(9), pp. 3537–3545.
[52] Kroll, M. H., Hellums, J. D., McIntire, L. V., Schafer, A. I., and Moake, J. L., 1996, "Platelets and Shear Stress," Blood, **88**(5), pp. 1525–1541.
[53] Slepian, M. J., Sheriff, J., Hutchinson, M., Tran, P., Bajaj, N., Garcia, J. G., Saavedra, S. S., and Bluestein, D., 2017, "Shear-Mediated Platelet Activation in the Free Flow: Perspectives on the Emerging Spectrum of Cell Mechano-biological Mechanisms Mediating Cardiovascular Implant Thrombosis," J. Biomech., **50**, pp. 20–25.
[54] Roka-Moiia, Y., Ammann, K. R., Miller-Gutierrez, S., Sweedo, A., Palomares, D., Italiano, J., Sheriff, J., Bluestein, D., and Slepian, M. J., 2021, "Shear-Mediated Platelet Activation in the Free Flow II: Evolving Mechanobiological Mechanisms Reveal an Identifiable Signature of Activation and a Bi-Directional Platelet Dyscrasia With Thrombotic and Bleeding Features," J. Biomech., **123**, p. 110415.
[55] Wurzinger, L., Opitz, R., Wolf, M., and Schmid-Schönbein, H., 1985, "'Shear Induced Platelet Activation'—A Critical Reappraisal," Biorheology, **22**(5), pp. 399–413.
[56] Wurzinger, L. J., 1990, "Histophysiology of the Circulating Platelet," Adv. Anat., Embryol., Cell Biol., **120**, pp. 1–96.
[57] Sheriff, J., Bluestein, D., Girdhar, G., and Jesty, J., 2010, "High-Shear Stress Sensitizes Platelets to Subsequent Low-Shear Conditions," Ann. Biomed. Eng., **38**(4), pp. 1442–1450.
[58] Goncalves, I., Nesbitt, W. S., Yuan, Y., and Jackson, S. P., 2005, "Importance of Temporal Flow Gradients and Integrin αIIbβ3 Mechanotransduction for Shear Activation of Platelets," J. Biol. Chem., **280**(15), pp. 15430–15437.
[59] Dorsam, R. T., and Kunapuli, S. P., 2004, "Central Role of the P2Y 12 Receptor in Platelet Activation," J. Clin. Invest., **113**(3), pp. 340–345.
[60] Schneider, S., Nuschele, S., Wixforth, A., Gorzelanny, C., Alexander-Katz, A., Netz, R., and Schneider, M. F., 2007, "Shear-Induced Unfolding Triggers Adhesion of von Willebrand Factor Fibers," Proc. Natl. Acad. Sci., **104**(19), pp. 7899–7903.
[61] Slaughter, M. S., Pagani, F. D., Rogers, J. G., Miller, L. W., Sun, B., Russell, S. D., Starling, R. C., et alet al., 2010, "Clinical Management of Continuous-Flow Left Ventricular Assist Devices in Advanced Heart Failure," J. Heart Lung Transplant., **29**(4), pp. S1–S39.
[62] Birks, E. J., 2010, "Left Ventricular Assist Devices," Heart, **96**(1), pp. 63–71.
[63] Almond, C. S., Singh, T. P., Gauvreau, K., Piercey, G. E., Fynn-Thompson, F., Rycus, P. T., Bartlett, R. H., and Thiagarajan, R. R., 2011, "Extracorporeal Membrane Oxygenation for Bridge to Heart Transplantation Among Children in the United States: Analysis of Data From the Organ Procurement and Transplant Network and Extracorporeal Life Support Organization Registry," Circulation, **123**(25), pp. 2975–2984.
[64] Abrams, D., Combes, A., and Brodie, D., 2014, "Extracorporeal Membrane Oxygenation in Cardiopulmonary Disease in Adults," J. Am. Coll. Cardiol., **63**(25), pp. 2769–2778.
[65] Sakota, D., Sakamoto, R., Sobajima, H., Yokoyama, N., Waguri, S., Ohuchi, K., and Takatani, S., 2008, "Mechanical Damage of Red Blood Cells by Rotary Blood Pumps: Selective Destruction of Aged Red Blood Cells and Subhemolytic Trauma," Artif. Organs, **32**(10), pp. 785–791.
[66] Sohrabi, S., and Liu, Y., 2017, "A Cellular Model of Shear-Induced Hemolysis," Artif. Organs, **41**(9), pp. E80–E91.
[67] van der Meer, F. J., Rosendaal, F. R., Vandenbroucke, J. P., and Briët, E., 1993, "Bleeding Complications in Oral Anticoagulant Therapy: An Analysis of Risk Factors," Arch. Intern. Med., **153**(13), pp. 1557–1562.
[68] Eckman, P. M., and John, R., 2012, "Bleeding and Thrombosis in Patients With Continuous-Flow Ventricular Assist Devices," Circulation, **125**(24), pp. 3038–3047.
[69] Schafer, A. I., 1984, "Bleeding and Thrombosis in the Myeloproliferative Disorders," Blood, **64**(1), pp. 1–12.
[70] Mokadam, N. A., Andrus, S., and Ungerleider, A., 2011, "Thrombus Formation in a HeartMate II," Eur. J. Cardio-Thorac. Surg., **39**(3), pp. 414–414.
[71] Chen, Z., Mondal, N. K., Ding, J., Gao, J., Griffith, B. P., and Wu, Z. J., 2015, "Shear-Induced Platelet Receptor Shedding by Non-Physiological High Shear Stress With Short Exposure Time: Glycoprotein Ibα and Glycoprotein VI," Thromb. Res., **135**(4), pp. 692–698.
[72] Behbahani, M., Behr, M., Hormes, M., Steinseifer, U., Arora, D., Coronado, O., and Pasquali, M., 2009, "A Review of Computational Fluid Dynamics Analysis of Blood Pumps," Eur. J. Appl. Math., **20**(4), pp. 363–397.
[73] Feng, R., Xenos, M., Girdhar, G., Kang, W., Davenport, J. W., Deng, Y., and Bluestein, D., 2012, "Viscous Flow Simulation in a Stenosis Model Using Discrete Particle Dynamics: A Comparison Between DPD and CFD," Biomech. Model. Mechanobiol., **11**(1–2), pp. 119–129.
[74] Wang, L., Chen, Z., Zhang, J., Zhang, X., and Wu, Z. J., 2020, "Modeling Clot Formation of Shear-Injured Platelets in Flow by a Dissipative Particle Dynamics Method," Bull. Math. Biol., **82**(7), p. 83.
[75] Ye, T., Phan-Thien, N., and Lim, C. T., 2016, "Particle-Based Simulations of Red Blood Cells—A Review," J. Biomech., **49**(11), pp. 2255–2266.
[76] Shahriari, S., Maleki, H., Hassan, I., and Kadem, L., 2012, "Evaluation of Shear Stress Accumulation on Blood Components in Normal and Dysfunctional Bileaflet Mechanical Heart Valves Using Smoothed Particle Hydrodynamics," J. Biomech., **45**(15), pp. 2637–2644.
[77] Godunov, S., and Bohachevsky, I., 1959, "Finite Difference Method for Numerical Computation of Discontinuous Solutions of the Equations of Fluid Dynamics," Mat. Sb., **47**(3), pp. 271–306.
[78] Moukalled, F., Mangani, L., and Darwish, M., 2016, *The Finite Volume Method in Computational Fluid Dynamics*, Springer, Berlin.
[79] Han, D., Liu, G. R., and Abdallah, S., 2019, "An Eulerian–Lagrangian–Lagrangian Method for Solving Thin Moving Rigid Body Immersed in the Fluid," Comput. Fluids, **179**, pp. 687–701.
[80] Han, D., Liu, G. R., and Abdallah, S., 2020, "An Eulerian-Lagrangian-Lagrangian Method for 2D Fluid-Structure Interaction Problem With a Thin Flexible Structure Immersed in Fluids," Comput. Struct., **228**, p. 106179.
[81] Han, D., Liu, G. R., and Abdallah, S., 2020, "An Eulerian-Lagrangian-Lagrangian Method for Solving Fluid-Structure Interaction Problems With Bulk Solids," J. Comput. Phys., **405**, p. 109164.
[82] Greifzu, F., Kratzsch, C., Forgber, T., Lindner, F., and Schwarze, R., 2016, "Assessment of Particle-Tracking Models for Dispersed Particle-Laden Flows Implemented in OpenFOAM and ANSYS FLUENT," Eng. Appl. Comput. Fluid Mech., **10**(1), pp. 30–43.
[83] Liu, M., Liu, G., Zhou, L., and Chang, J., 2015, "Dissipative Particle Dynamics (DPD): An Overview and Recent Developments," Arch. Comput. Methods Eng., **22**(4), pp. 529–556.
[84] Tosenberger, A., Ataullakhanov, F., Bessonov, N., Panteleev, M., Tokarev, A., and Volpert, V., 2013, "Modelling of Thrombus Growth in Flow With a DPD-PDE Method," J. Theor. Biol., **337**, pp. 30–41.
[85] Gao, C., Zhang, P., Marom, G., Deng, Y., and Bluestein, D., 2017, "Reducing the Effects of Compressibility in DPD-Based Blood Flow Simulations Through Severe Stenotic Microchannels," J. Comput. Phys., **335**, pp. 812–827.
[86] Zhang, H., Tan, Y., Shu, S., Niu, X., Trias, F. X., Yang, D., Li, H., and Sheng, Y., 2014, "Numerical Investigation on the Role of Discrete Element Method in Combined LBM–IBM–DEM Modeling," Comput. Fluids, **94**, pp. 37–48.
[87] Cheng, L., Tan, J., Yun, Z., Wang, S., and Yu, Z., 2021, "Analysis of Flow Field and Hemolysis Index in Axial Flow Blood Pump by Computational Fluid Dynamics–Discrete Element Method," Int. J. Artif. Organs, **44**(1), pp. 46–54.
[88] Miyazaki, H., and Yamaguchi, T., 2003, "Formation and Destruction of Primary Thrombi Under the Influence of Blood Flow and von Willebrand Factor Analyzed by a Discrete Element Method," Biorheology, **40**(1, 2, 3), pp. 265–272.
[89] Apel, J., Paul, R., Klaus, S., Siess, T., and Reul, H., 2001, "Assessment of Hemolysis Related Quantities in a Microaxial Blood Pump by Computational Fluid Dynamics," Artif. Organs, **25**(5), pp. 341–347.
[90] Bludszuweit, C., 1995, "Three-Dimensional Numerical Prediction of Stress Loading of Blood Particles in a Centrifugal Pump," Artif. Organs, **19**(7), pp. 590–596.
[91] Faghih, M. M., and Keith Sharp, M., 2016, "Extending the Power-Law Hemolysis Model to Complex Flows," ASME J. Biomech. Eng., **138**(12), p. 124504.
[92] Faghih, M. M., and Sharp, M. K., 2019, "On Eulerian Versus Lagrangian Models of Mechanical Blood Damage and the Linearized Damage Function," Artif. Organs, **43**(7), pp. 681–687.
[93] Goubergrits, L., 2006, "Numerical Modeling of Blood Damage: Current Status, Challenges and Future Prospects," Expert Rev. Med. Devices, **3**(5), pp. 527–531.
[94] Grigioni, M., Daniele, C., Morbiducci, U., D'Avenio, G., Di Benedetto, G., and Barbaro, V., 2004, "The Power-Law Mathematical Model for Blood Damage Prediction: Analytical Developments and Physical Inconsistencies," Artif. Organs, **28**(5), pp. 467–475.
[95] Sheriff, J., Soares, J. S., Xenos, M., Jesty, J., and Bluestein, D., 2013, "Evaluation of Shear-Induced Platelet Activation Models Under Constant and Dynamic Shear Stress Loading Conditions Relevant to Devices," Ann. Biomed. Eng., **41**(6), pp. 1279–1296.
[96] Garon, A., and Farinas, M. I., 2004, "Fast Three-Dimensional Numerical Hemolysis Approximation," Artif. Organs, **28**(11), pp. 1016–1025.
[97] Grigioni, M., Morbiducci, U., D'Avenio, G., Di Benedetto, G., and Del Gaudio, C., 2005, "A Novel Formulation for Blood Trauma Prediction by a Modified Power-Law Mathematical Model," Biomech. Model. Mechanobiol., **4**(4), pp. 249–260.
[98] Liu, G.-M., Jin, D.-H., Chen, H.-B., Hou, J.-F., Zhang, Y., Sun, H.-S., Zhou, J.-Y., Hu, S.-S., and Gui, X.-M., 2019, "Numerical Investigation of the Influence of a Bearing/Shaft Structure in an Axial Blood Pump on the Potential for Device Thrombosis," Int. J. Artif. Organs, **42**(4), pp. 182–189.
[99] Yin, W., Alemu, Y., Affeld, K., Jesty, J., and Bluestein, D., 2004, "Flow-Induced Platelet Activation in Bileaflet and Monoleaflet Mechanical Heart Valves," Ann. Biomed. Eng., **32**(8), pp. 1058–1066.
[100] Chiu, W.-C., Girdhar, G., Xenos, M., Alemu, Y., Soares, J. S., Einav, S., Slepian, M., and Bluestein, D., 2014, "Thromboresistance Comparison of the HeartMate II Ventricular Assist Device With the Device Thrombogenicity Emulation-Optimized HeartAssist 5 VAD," ASME J. Biomech. Eng., **136**(2), p. 021014.
[101] Soares, J. S., Sheriff, J., and Bluestein, D., 2013, "A Novel Mathematical Model of Activation and Sensitization of Platelets Subjected to Dynamic Stress Histories," Biomech. Model. Mechanobiol., **12**(6), pp. 1127–1141.
[102] Hedayat, M., and Borazjani, I., 2019, "Comparison of Platelet Activation Through Hinge Vs Bulk Flow in Bileaflet Mechanical Heart Valves," J. Biomech., **83**, pp. 280–290.
[103] Hedayat, M., Asgharzadeh, H., and Borazjani, I., 2017, "Platelet Activation of Mechanical Versus Bioprosthetic Heart Valves During Systole," J. Biomech., **56**, pp. 111–116.
[104] Consolo, F., Sheriff, J., Gorla, S., Magri, N., Bluestein, D., Pappalardo, F., Slepian, M. J., Fiore, G. B., and Redaelli, A., 2017, "High Frequency Components of Hemodynamic Shear Stress Profiles Are a Major Determinant of

Shear-Mediated Platelet Activation in Therapeutic Blood Recirculating Devices," Sci. Rep., **7**(1), p. 4994.
[105] Yeleswarapu, K. K., Antaki, J. F., Kameneva, M. V., and Rajagopal, K. R., 1995, "A Mathematical Model for Shear-Induced Hemolysis," Artif. Organs, **19**(7), pp. 576–582.
[106] Anand, M., Rajagopal, K., and Rajagopal, K., 2003, "A Model Incorporating Some of the Mechanical and Biochemical Factors Underlying Clot Formation and Dissolution in Flowing Blood," J. Theor. Med., **5**(3–4), pp. 183–218.
[107] Anand, M., Rajagopal, K., and Rajagopal, K., 2005, "A Model for the Formation and Lysis of Blood Clots," Pathophysiol. Haemostasis Thromb., **34**(2–3), pp. 109–120.
[108] Fogelson, A. L., and Neeves, K. B., 2015, "Fluid Mechanics of Blood Clot Formation," Annu. Rev. Fluid Mech., **47**(1), pp. 377–403.
[109] Fogelson, A. L., 1984, "A Mathematical Model and Numerical Method for Studying Platelet Adhesion and Aggregation During Blood Clotting," J. Comput. Phys., **56**(1), pp. 111–134.
[110] Chesnutt, J. K., and Han, H.-C., 2011, "Tortuosity Triggers Platelet Activation and Thrombus Formation in Microvessels," ASME J. Biomech. Eng., **133**(12), p. 121004.
[111] Chesnutt, J. K., and Han, H.-C., 2015, "Simulation of the Microscopic Process During Initiation of Stent Thrombosis," Comput. Biol. Med., **56**, pp. 182–191.
[112] Feng, Z.-G., Cortina, M., Chesnutt, J. K., and Han, H.-C., 2017, "Numerical Simulation of Thrombotic Occlusion in Tortuous Arterioles," J. Cardiol. Cardiovasc. Med., **2**(1), pp. 95–111.
[113] de Oliveira, D. C., Owen, D. G., Qian, S., Green, N. C., Espino, D. M., and Shepherd, D. E., 2021, "Computational Fluid Dynamics of the Right Atrium: Assessment of Modelling Criteria for the Evaluation of Dialysis Catheters," PLoS One, **16**(2), p. e0247438.
[114] Chesnutt, J. K., and Han, H.-C., 2013, "Effect of Red Blood Cells on Platelet Activation and Thrombus Formation in Tortuous Arterioles," Front. Bioeng. Biotechnol., **1**, p. 18.
[115] Pushin, D. M., Salikhova, T. Y., Zlobina, K. E., and Guria, G. T., 2020, "Platelet Activation Via Dynamic Conformational Changes of von Willebrand Factor Under Shear," PLoS One, **15**(6), p. e0234501.
[116] Bark, D. L., Jr., and Ku, D. N., 2010, "Wall Shear Over High Degree Stenoses Pertinent to Atherothrombosis," J. Biomech., **43**(15), pp. 2970–2977.
[117] Goodman, P. D., Barlow, E. T., Crapo, P. M., Mohammad, S. F., and Solen, K. A., 2005, "Computational Model of Device-Induced Thrombosis and Thromboembolism," Ann. Biomed. Eng., **33**(6), pp. 780–797.
[118] Tambasco, M., and Steinman, D. A., 2003, "Path-Dependent Hemodynamics of the Stenosed Carotid Bifurcation," Ann. Biomed. Eng., **31**(9), pp. 1054–1065.
[119] Zhang, P., Zhang, N., Deng, Y., and Bluestein, D., 2015, "A Multiple Time Stepping Algorithm for Efficient Multiscale Modeling of Platelets Flowing in Blood Plasma," J. Comput. Phys., **284**, pp. 668–686.
[120] Wu, J., Yun, B. M., Fallon, A. M., Hanson, S. R., Aidun, C. K., and Yoganathan, A. P., 2011, "Numerical Investigation of the Effects of Channel Geometry on Platelet Activation and Blood Damage," Ann. Biomed. Eng., **39**(2), pp. 897–910.
[121] Morbiducci, U., Ponzini, R., Nobili, M., Massai, D., Montevecchi, F. M., Bluestein, D., and Redaelli, A., 2009, "Blood Damage Safety of Prosthetic Heart Valves. Shear-Induced Platelet Activation and Local Flow Dynamics: A Fluid–Structure Interaction Approach," J. Biomech., **42**(12), pp. 1952–1960.
[122] Alemu, Y., Xenos, M., Deng, Y., Feng, R., Einav, S., and Bluestein, D., 2008, "Damage Accumulation Model of Prosthetic Heart Valves in Forward and Reverse Flow Phases," ASME Paper No. SBC2008-193010.
[123] Hansen, K. B., Arzani, A., and Shadden, S. C., 2015, "Mechanical Platelet Activation Potential in Abdominal Aortic Aneurysms," ASME J. Biomech. Eng., **137**(4), p. 041005.
[124] Zlobina, K., and Guria, G. T., 2016, "Platelet Activation Risk Index as a Prognostic Thrombosis Indicator," Sci. Rep., **6**(1), p. 30508.
[125] Tan, J., Thomas, A., and Liu, Y., 2012, "Influence of Red Blood Cells on Nanoparticle Targeted Delivery in Microcirculation," Soft Matter, **8**(6), pp. 1934–1946.
[126] Liu, Y., and Liu, W. K., 2006, "Rheology of Red Blood Cell Aggregation by Computer Simulation," J. Comput. Phys., **220**(1), pp. 139–154.
[127] Závodszky, G., van Rooij, B., Azizi, V., and Hoekstra, A., 2017, "Cellular Level In-Silico Modeling of Blood Rheology With an Improved Material Model for Red Blood Cells," Front. Physiol., **8**, p. 563.
[128] Thon, J. N., Macleod, H., Begonja, A. J., Zhu, J., Lee, K.-C., Mogilner, A., Hartwig, J. H., and Italiano, J. E., 2012, "Microtubule and Cortical Forces Determine Platelet Size During Vascular Platelet Production," Nat. Commun., **3**(1), p. 852.
[129] van Dijk, J., Bompard, G., Cau, J., Kunishima, S., Rabeharivelo, G., Mateos-Langerak, J., Cazevieille, C., et alet al., 2018, "Microtubule Polyglutamylation and Acetylation Drive Microtubule Dynamics Critical for Platelet Formation," BMC Biol., **16**(1), p. 116.
[130] Moskalensky, A. E., and Litvinenko, A. L., 2019, "The Platelet Shape Change: Biophysical Basis and Physiological Consequences," Platelets, **30**(5), pp. 543–548.
[131] Dmitrieff, S., Alsina, A., Mathur, A., and Nédélec, F. J., 2017, "Balance of Microtubule Stiffness and Cortical Tension Determines the Size of Blood Cells With Marginal Band Across Species," Proc. Natl. Acad. Sci., **114**(17), pp. 4418–4423.
[132] Sheriff, J., and Bluestein, D., 2019, "Platelet Dynamics in Blood Flow," Dynamics of Blood Cell Suspensions in Microflows, CRC Press, Boca Raton, FL, pp. 215–256.